

## Density of states near the Fermi level from measurements of variable-range-hopping magnetoresistance in germanium

I. S. Shlimak

*The Jack and Pearl Resnick Institute for Advanced Technology and Department of Physics,  
Bar-Ilan University, Ramat-Gan, Israel*

M. J. Lea, P. Fozooni, and P. Stefanyi

*Department of Physics, Royal Holloway, University of London, Egham, Surrey TW20 0EX, England*

A. N. Ionov

*A. F. Ioffe Physico-Technical Institute, Russian Academy of Sciences, St. Petersburg 194021, Russia*

(Received 26 January 1993; revised manuscript received 25 May 1993)

The variable-range-hopping (VRH) resistance of  $n$ - and  $p$ -type neutron-transmutation-doped (NTD) Ge was measured at temperatures down to 30 mK and in magnetic fields up to 7 T. It is shown that the temperature dependence of the VRH resistance can be reduced to a universal curve for all samples and fields, from which one can determine the density of states (DOS) near the Fermi level. Temperature-dependent measurements show that VRH conductivity at low energies is in agreement with the existence of a soft Coulomb gap at the Fermi level. The tendency to a constant DOS at higher energies is shown: the so-called crossover phenomenon in VRH conductivity which reduces the effect of the Coulomb gap at higher magnetic fields and temperatures is discussed.

### INTRODUCTION

It is well established<sup>1</sup> that the resistance of an Anderson insulator at low temperatures follows Mott's law for variable range hopping (VRH):

$$R = R_0 \exp[(T_0/T)^p], \quad (1)$$

where  $T_0$  and the exponent  $p$  depend on the density of states (DOS)  $g(E)$  close to the Fermi energy  $E_F$ . For a constant or slowly varying DOS,  $g(E) = g(E_F)$ , we have

$$p = \frac{1}{4}, \quad T_0 \equiv T_{1/4} = C_1 [g(E_F) a^3]^{-1}, \quad (2)$$

where  $a$  is the localization radius of the electron wave function and  $C_1 = 21$ .

Taking into account the Coulomb interaction between localized carriers, a parabolic "soft" gap appears at the Fermi energy:  $g(E_F) = 0$ ;  $g(E) = g_0(E - E_F)^2 = g_0 \epsilon^2$ . In this case we have the Efros-Shklovskii law<sup>1</sup>

$$p = \frac{1}{2}, \quad T_0 \equiv T_{1/2} = C_2 \frac{e^2}{\kappa a}, \quad (3)$$

where  $\kappa$  is the dielectric constant,  $e$  is the electronic charge,  $C_2 = 2.8$ , and

$$g_0 = 3/\pi(e^2/\kappa)^{-3}. \quad (4)$$

There are many observations of VRH resistivity in both of these regimes:  $p = \frac{1}{2}$  and  $\frac{1}{4}$ .<sup>2</sup> Recently attention has focused on crossover phenomenon and the transition from the first to the second regime with increasing temperature (see, for example, Ref. 3 and references therein). The Coulomb interaction can perturb the DOS only near the Fermi energy. Far from the Fermi level

( $|E - E_F| = |\epsilon| \gg E_F$ ) the DOS returns to its unperturbed value, which is approximately equal to  $g(E_F)$ . Hence, the half-width  $\Delta$  of the Coulomb gap (CG) can be determined from the equality

$$g_0 \Delta^2 = g(E_F), \quad \Delta = [g(E_F)/g_0]^{1/2}. \quad (5)$$

At low temperatures ( $T \ll \Delta$ ) the " $T^{-1/2}$  law," Eq. (3), must be observed. In the opposite limit ( $T \gg \Delta$ )  $p$  must be equal to  $\frac{1}{4}$ . The transition between these two regimes as the temperature or magnetic field is varied is the so-called crossover phenomenon. In Ref. 3 the crossover phenomenon was studied in  $n$ -type germanium in strong magnetic fields. In this paper we show that one can determine the shape of the DOS in  $n$ - and  $p$ -type Ge from measurements of the resistance and magnetoresistance in the VRH regime.

### EXPERIMENTAL RESULTS

Four samples of crystalline Ge were doped by the neutron-transmutation-doping (NTD) technique, which allows one to control the concentration of impurities and the degree of compensation with high accuracy. In the NTD method three of the five stable isotopes of Ge:  $^{70}\text{Ge}$ ,  $^{74}\text{Ge}$ , and  $^{76}\text{Ge}$  are transmuted by nuclear reactions with thermal neutrons into the impurity atoms  $^{71}\text{Ga}$  (shallow acceptor),  $^{75}\text{As}$  (shallow donor), and  $^{77}\text{Se}$  (deep donor). The concentration of impurities in the NTD method is proportional to the thermal-neutron dose or time of irradiation in the case of a constant neutron flux. The degree of compensation  $K$  is determined by the thermal-neutron cross section and the abundance of the isotopes which transform into dopant impurities. For

TABLE I. Isotopic composition of Ge samples.

Isotope	70	72	73	74	76
Natural Ge (%)	20.5	27.4	7.7	36.9	7.7
Ge-2(%)	1.7	2.4	1.0	93.9	1.0

isotopically natural Ge the NTD technique leads to the creation of  $p$ -type Ge with  $K$  between 30% and 40%.<sup>4</sup> This variation is due to the different dependences of the cross sections on neutron energy and hence  $K$  depends on the specific neutron energy spectrum used for irradiation. In order to obtain  $n$ -type Ge with small  $K$  a specially grown crystal, Ge-1, was previously used, enriched to 98% of the isotope  $^{74}\text{Ge}$ .<sup>5</sup> In this present work another crystal, Ge-2, was used, enriched to 93.9% of  $^{74}\text{Ge}$ . The isotopic compositions of natural Ge and of the Ge-2 crystal are shown in Table I.

As a result of the NTD of Ge-2 a series of three  $n$ -Ge(As) samples (numbers 6, 350, and 8) were obtained with small  $K$ . This compensation is connected with the existence of the small amount of the isotope  $^{70}\text{Ge}$  (1.7%), which transforms into gallium acceptor atoms. According to Ref. 6 the cross sections for  $^{70}\text{Ge}$  and  $^{74}\text{Ge}$  are 3.25 and 0.52 b. For thermal neutrons this would give  $K = 11\%$  for samples made from Ge-2. However, we estimate a slightly smaller compensation,  $K = 9\%$ , because of corrections based on the actual energy spectrum in the nuclear reactor used.<sup>7</sup> After irradiation the samples were

annealed at 420°C for 24 h at  $10^{-5}$  Torr. This relatively low annealing temperature protects against the diffusion of Cu and other rapidly diffusing impurities. Ohmic contacts to the  $n$ -Ge were prepared by alloying with In + 2% As at 300°C in a vacuum of  $10^{-5}$  Torr for 5 min. Sample H19 was processed and supplied by Professor E. E. Haller. It was prepared by the neutron irradiation of isotropically natural Ge using ultrapure starting material (with residual donor and acceptor concentrations,  $N_D, N_A < 10^{11} \text{ cm}^{-3}$ ). Electrical contacts to the  $p$ -Ge were made by implanting with  $\text{B}^+$  ions to a depth of 200 nm. The flux of  $\text{B}^+$  was about  $3 \times 10^{14} \text{ cm}^{-2}$ , enough to cause the implanted layers to become metallic. After the boron implantation, a layer of Pd about 20 nm thick was sputtered, followed by a Au film 400 nm thick. Finally the implanted layer was activated by annealing at 250°C for 1 h. The Ohmic behavior of the contacts was checked at low temperatures.

The samples were mounted carefully to minimize stresses and strains. The natural Ge sample was in the form of a rectangular plate,  $3 \times 3 \times 0.3$  mm. The plate was mounted horizontally in a slit copper rod on a thin sheet of paper with GE varnish to provide electrical isolation on a mechanically weak substrate. The plate overhung the edge of the slit so that 20- $\mu\text{m}$  gold leads could be bonded to the gold plating on the top and bottom faces. The enriched Ge samples were in bar form (typically  $1 \times 1 \times 9$  mm) and were held on a pure silicon

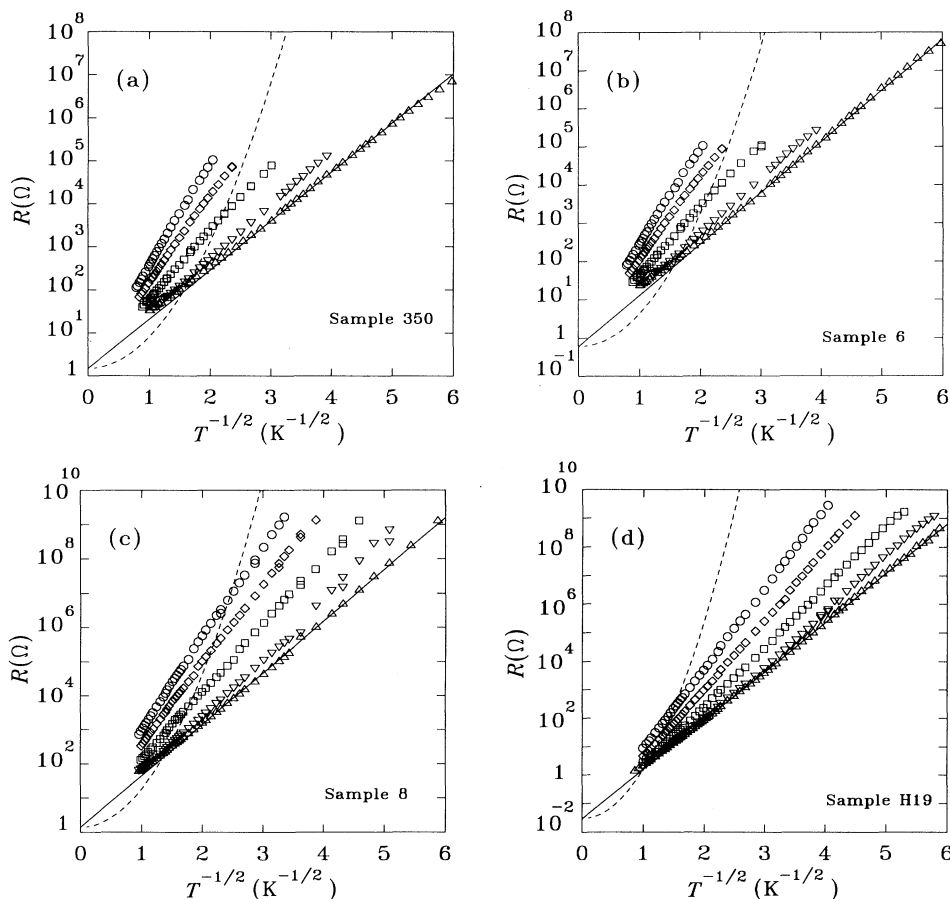


FIG. 1. The resistance of samples 350 (a), 6 (b), 8 (c), and H19 (d) in the VRH regime in zero magnetic field ( $\Delta$ ) and in magnetic fields of 1 ( $\nabla$ ), 3 ( $\square$ ), 5 ( $\diamond$ ), and 7 ( $\circ$ ) T. The solid lines show the fit to the  $T^{-1/2}$  law in the low-temperature, zero-field limit. The dashed lines show the center of the crossover region at  $T_c$  as discussed in the text.

substrate with GE varnish and paper over part of the lower face or free mounted with the leads acting as support. The samples were thermally anchored via the leads to copper strips anchored in turn to a copper rod screwed into the mixing chamber of a dilution refrigerator.

The resistance was measured by the four-probe method using both ac and dc techniques. For samples 6 and 350 a constant current source was used with Keithley 195 and 199 multimeters and an AVS-45 AS (25 Hz) resistance bridge. For samples 8 and H19, the electrical system was improved by using twisted pairs for the cryostat leads and a Keithley 236 voltage-current source-measure unit. As a result, resistances  $> 10^9 \Omega$  could be measured in high magnetic fields.

Figures 1(a), 1(b), 1(c), and 1(d) show the temperature dependence of the resistance of all four samples in zero field and in magnetic fields of 1, 3, 5, and 7 T. One can see a large positive magnetoresistance. At first sight all the data are in reasonable agreement with a “ $T^{-1/2}$  law,” Eq. (3). From this approach the magnetic field increases  $T_{1/2}$  while the factor  $R_0$  in Eq. (1) remains approximately constant. However, further analysis showed that the ex-

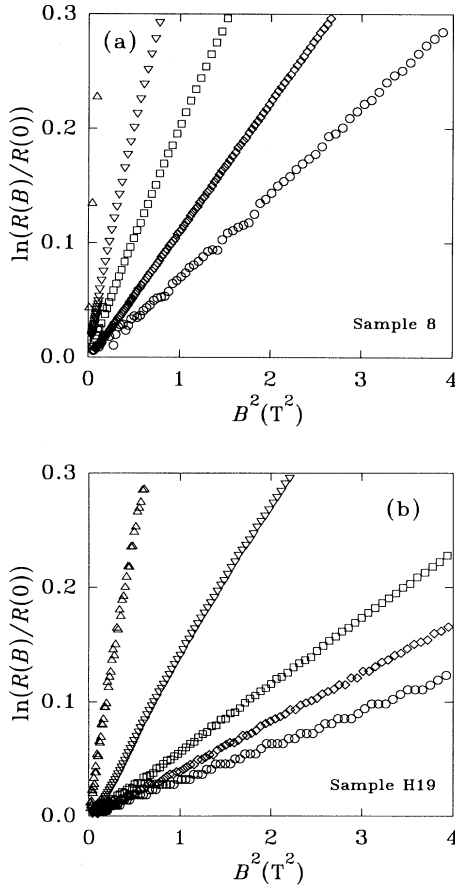


FIG. 2. (a) Magnetoresistance in weak magnetic fields for sample 8 at different temperatures: 1.037 K ( $\circ$ ), 0.720 K ( $\diamond$ ), 0.500 K ( $\square$ ), 0.320 K ( $\nabla$ ), and 0.101 K ( $\triangle$ ). (b) Magnetoresistance in weak magnetic fields for sample H19 at different temperatures: 1.00 K ( $\circ$ ), 0.700 K ( $\diamond$ ), 0.500 K ( $\square$ ), 0.250 K ( $\nabla$ ), and 0.120 K ( $\triangle$ ).

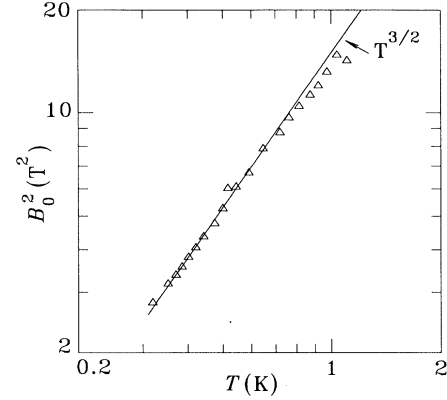


FIG. 3. Dependence of the parameter  $B_0$  on  $T$  for sample 8. The solid shows the  $T^{3/2}$  dependence.

ponent  $p$  in Eq. (1) shifts to lower values, particularly at higher temperatures, with increasing  $B$ . For samples 6 and 350  $p$  shifted from  $\frac{1}{2}$  to almost  $\frac{1}{3}$ ,<sup>3</sup> while for sample 8 the change is smaller. For sample H19  $p$  remains close to  $\frac{1}{2}$  even at strong fields, as also observed by Schoepe for a Ge thermoresistor.<sup>8</sup> We shall see below that the “ $T^{-1/2}$  law” is only strictly valid in the low-temperature limit in zero magnetic field.

In weak magnetic fields the magnetoresistance (MR) of all the samples studied is closely proportional to  $\exp((B/B_0)^2)$  or

$$\ln \left[ \frac{R(B)}{R(0)} \right] = \left[ \frac{B}{B_0} \right]^2 \quad (6)$$

as shown in Fig. 2(a) for sample 8 and in Fig. 2(b) for sample H19 at several temperatures. The temperature dependence of the parameter  $B_0$  is shown in Fig. 3 for sample 8. This dependence can be described as  $B_0^2 \sim T^m$ , where  $m = 1.5$  in the low-temperature limit as shown by the solid line in the figure. In intermediate and strong magnetic fields the power in Eq. (6) decreases continuously from 2 to 1 or lower, as discussed below (see Fig. 4).

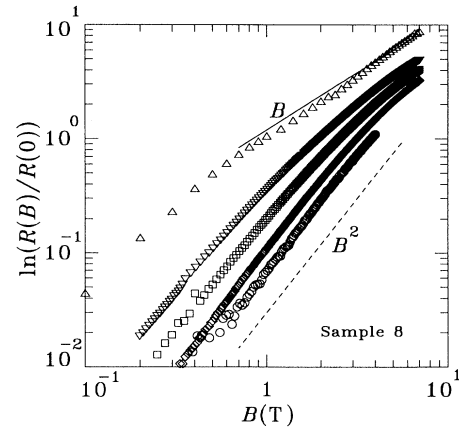


FIG. 4. Magnetoresistance of sample 8 as a function of magnetic field at different temperatures: 1.037 K ( $\circ$ ), 0.720 K ( $\diamond$ ), 0.500 K ( $\square$ ), 0.320 K ( $\nabla$ ), and 0.101 K ( $\triangle$ ). The solid line shows  $\ln(R) \propto B$  and the dashed line shows  $\ln(R) \propto B^2$ .

## DISCUSSION

It has been shown in Refs. 9 and 10 that measurements of the VRH resistivity in the CG regime, Eq. (3), combined with the magnetoresistance in weak fields allow one to determine many important parameters concerning the structure of the electronic wave function and the DOS near  $E_F$ , such as the localization radius  $a$ , the dielectric constant  $\kappa$ , and  $g_0$ . First the low-temperature limit of the zero-field data is fitted to the " $T^{-1/2}$  law" to obtain values of  $T_{1/2}$  and  $R_0$  as shown in Table II. The geometrical factor  $L$  used to convert resistance  $R$  to resistivity  $\rho=LR$  was 0.03 m for the disk-shaped H19 sample and  $(2\pm 0.5)\times 10^{-4}$  m for samples 6, 350, and 8.

The localization radius  $a$  can be extracted from the slope of  $B_0^2$  vs  $T^{3/2}$  in the low temperature, or Coulomb gap, limit:

$$B_0^2 = \left[ \frac{C_3 \hbar^2}{e^2 a^4} \right] \left[ \frac{T}{T_{1/2}} \right]^{3/2}, \quad (7)$$

where the numerical factor  $C_3=660$  (Ref. 1) or 288 (Ref. 8), depending on the theoretical assumptions used. A knowledge of  $T_{1/2}$  in zero field and  $a$  then allows one to determine  $\kappa$  from Eq. (3) and  $g_0$  from Eq. (4), as shown in Table II.

Near the metal-insulator transition (MIT) these values of  $a$  and  $\kappa$  are much larger than the Bohr radius for an individual shallow impurity center  $a_0$  and the static dielectric constant  $\kappa_0$  in undoped Ge because of the nearness to the transition:<sup>1</sup>

$$a = a_0 [1 - (N/N_c)]^{-\nu}, \quad \kappa = \kappa_0 [1 - (N/N_c)]^{-\xi}, \quad (8)$$

where  $N_c$  is the critical concentration of the MIT, and  $\nu$  and  $\xi$  are critical indices. Assuming that  $\kappa_0=16$  for Ge one can determine the scaling factor  $z = \kappa/\kappa_0$ . According to scaling theory<sup>11,12</sup> and experimental observation<sup>10</sup>  $\xi/\nu=2$  and consequently we have  $a_0 = a/z^{1/2}$  which enables the effective Bohr radius  $a_0$  to be determined for our samples, without explicit knowledge of  $N$  or  $N_c$ . The results of this analysis are presented in Table II. We used  $C_3=288$  as the more reliable value for weak and intermediate magnetic fields<sup>8</sup> (if  $C_3=660$  is used the values of  $a$  and  $a_0$  would be increased by 23%). For the enriched Ge samples, the values of  $N$  were in the range from  $2.7$  to  $3.2 \times 10^{17} \text{ cm}^{-3}$  while  $N_c = (3.4 \pm 0.2) \times 10^{17} \text{ cm}^{-3}$  has been estimated previously.<sup>13</sup>

It is interesting to note that for all three samples with As as the majority impurity the values of the Bohr radius

$a_0$  obtained by this analysis are the same. It was a surprise that  $a_0$  for the acceptor impurity Ga (sample H19) was smaller, only 4.0 nm, because for lightly doped Ge  $\langle \text{Ga} \rangle a_0 = 9.0 \text{ nm}$ .<sup>14</sup> This can be explained as follows. According to Ref. 14, the value of  $a$  in the tail of the wave function  $\Psi(r)$  in  $p$ -Ge is determined by light holes. The exact wave function of holes localized on shallow acceptors in Ge is not known but, at high acceptor concentrations, the overlap integral has a maximum closer to the central part of the wave function, where the effective mass of heavy holes determines the value of  $a$  (the concentration of heavy holes is 97% of the total concentration; in the limit  $a=3 \text{ nm}$ ). It is interesting that the value of  $a_0=4.0 \text{ nm}$  was found by Schoepe<sup>8</sup> for a Ge sample with unknown doping, which suggests that that sample was also  $p$ -type (though Schoepe suggested As doping as the most likely). The absolute values of the above parameters depend on the numerical constants  $C_2$  and  $C_3$ . However, the correlation between the values for different samples are good and support the theoretical calculations.

Let us turn to the determination of the DOS, based on the analysis presented by Schoepe.<sup>8</sup> In contrast with nearest-neighbor hopping conductivity the VRH mechanism involves only some of the localized states around the Fermi level, the so-called "optimal band." The lower the  $T$  is, the narrower is this "optimal band" whose half-width  $E_c$  is given by  $E_c \sim T^{1-p} = T\xi_c$  (Ref. 1) where  $\xi_c = (T_0/T)^p$  is the critical percolation parameter. The value of  $\xi_c(T) = \ln[R(T)/R_0]$  can be obtained from the experimental data. The mean hopping distance  $r(T) = [I(E_c)]^{-1/3}$  where  $I(E_c)$  is the integrated density of localized states:

$$I(E_c) = \int_{-E_c}^{E_c} g(\epsilon) d\epsilon = 2 \int_0^{E_c} g(\epsilon) d\epsilon. \quad (9)$$

On the other hand,  $r(T) = a\xi_c/2$  (Ref. 1), and the average hopping volume around each site is

$$V(\xi_c) = \frac{4\pi}{3} \left[ \frac{a\xi_c}{2} \right]^3. \quad (10)$$

The number of sites within  $N(\xi_c)$ , which is the critical one for the formation of a percolation path, is given by

$$n_c = I(E_c) V(\xi_c), \quad (11)$$

where  $n_c$  has the value 7.66 from percolation theory.<sup>1</sup> For a constant DOS at the Fermi level  $I(E_c)$  is a linear

TABLE II. VRH parameters for Ge samples.

Sample	$R_0$ ( $\Omega$ )	$T_{1/2}$ (K)	$a$ (nm)	$\kappa$	$a_0$ (nm)	$g_0$ ( $\text{cm}^{-3} \text{ K}^{-3}$ )	$\Delta$ (K)	$g(E_F)$ ( $\text{cm}^{-3} \text{ K}^{-1}$ )
350	1.5	6.9	26.6	254	6.7	$3.5 \times 10^{15}$	1.7	$10 \times 10^{15}$
6	0.6	9.5	24.0	205	6.7	$1.8 \times 10^{15}$	2.0	$7 \times 10^{15}$
8	1.4	12.1	21.9	176	6.6	$1.2 \times 10^{15}$	2.6	$8 \times 10^{15}$
H19	0.03	15.7	14.4	206	4.0	$1.9 \times 10^{15}$	4.0	$30 \times 10^{15}$

function of  $E_c$ :

$$I(E_c) = 2g(E_F)E_c. \quad (12)$$

In the opposite case, within the CG,  $g(E) = g_0\varepsilon^2$  which leads to a cubic dependence:

$$I(E_c) = \frac{2}{3}g_0E_c^3. \quad (13)$$

The general form of the DOS must have two limits, depending on the relation between the energy of the "optimal gap"  $2E_c$  and the width of the CG,  $2\Delta$ : for  $E_c \ll \Delta$ ,  $g(\varepsilon) \sim \varepsilon^2$ , and if  $E_c \gg \Delta$ ,  $g(\varepsilon) = g(E_F)$ . Let us assume an expression of the form

$$g(\varepsilon) = \frac{g_0\varepsilon^2}{1 + (\varepsilon/\Delta)^2}, \quad (14)$$

where  $\Delta$  is determined from Eq. (5). Substituting Eq. (14) into Eq. (9) one obtains

$$I(E_c) = 2g_0\Delta^2 \{ (E_c/\Delta) - \arctan(E_c/\Delta) \}, \quad (15)$$

which in the two limits gives

$$I(E_c) = \frac{2}{3}g_0E_c^3, \quad E_c \ll \Delta, \quad (16)$$

$$I(E_c) = 2g_0\Delta^3 \{ (E_c/\Delta) - (\pi/2) \}, \quad E_c \gg \Delta. \quad (17)$$

One can see that Eq. (16) is equal to Eq. (13) and also Eq. (17) is equal to Eq. (12) minus a term  $\pi g_0\Delta^3$  because of the existence of the CG at the Fermi energy. The general expression Eq. (15) demonstrates an extended crossover phenomenon: a smooth transition from a cubic to a linear dependence of  $I(E_c)$ . [Other expressions for  $g(\varepsilon)$  could be selected; Eq. (14) is essentially an interpolation formula between the constant DOS and CG regimes.] In Ref. 3 the crossover phenomenon was characterized by a critical temperature  $T_c$  determined from the equality of the "optimal band" width  $2E_c$  and the width of the Coulomb gap  $2\Delta$ :  $\Delta = E_c(T_c) = T_c\xi_c$ . From this condition the CG regime must be observed at  $T < T_c$  and the regime of constant DOS at  $T > T_c$  (note that  $T_c$  will, in general, be field dependent). It is clear, however, that the crossover is a continuous process, depending on the sharpness of the transition from a CG to a constant DOS and therefore the value of  $T_c$  corresponds approximately to the middle point of this phenomenon. If the half-width  $\Delta$  of the Coulomb gap is known, then a simple graphic method can be used for the determination of  $T_c$  and to demonstrate its field dependence due to magnetoresistance. Let us introduce a critical resistance  $R_c = R(T_c)$  at a given temperature  $T_c$ . Since  $\xi_c(T_c) = \ln(R_c/R_0)$  we obtain  $R_c = R_0 \exp(\Delta/T_c)$ . Hence a plot of  $R_c$  versus  $T_c$  is a parabola on a graph of  $\ln R$  or  $\log_{10} R$  versus  $T^{-1/2}$ , as shown as a dashed line in Figs. 1(a)–1(d) for each sample, using values of  $\Delta$  obtained as described below. The crossing points of this parabola with the experimental data for  $R(B, T)$  indicate the values of  $T_c$  and  $R_c$  for each magnetic field. Data which lie above this line are in the constant DOS regime while data below the line are in the CG regime. It can be seen that the crossover temperature effectively decreases with field as  $\xi_c$  increases due to magnetoresistance, as dis-

cussed in Ref. 3. An extended crossover effect was also suggested in Ref. 15.

In order to obtain  $I(E_c)$  from the experimental data of  $R(T)$  in zero field we proceed as follows. The low-temperature limit of the data is fitted to the Coulomb gap " $T^{-1/2}$  law" to obtain  $T_{1/2}$  and  $R_0$  as in Table II. Hence we can find  $\xi_c(T) = \ln[R(T)/R_0]$  at any temperature  $T$ . The integrated density of states  $I(E_c)$  is then given by

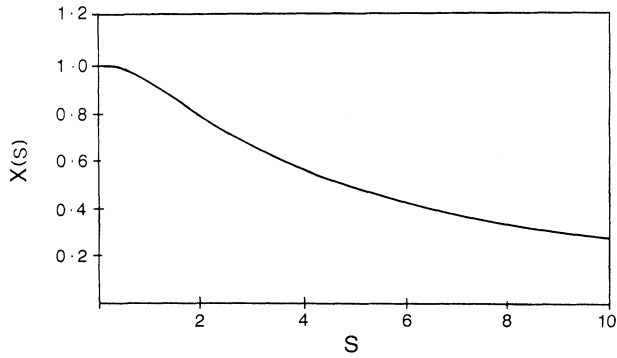
$$I(E_c) = \frac{6n_c}{\pi} \frac{1}{a^3} \frac{1}{(\xi_c(T))^3}, \quad (18)$$

where  $a$  is given in Table II. This expression is valid within this model at all temperatures, not just in the low-temperature limit. The energy scale is given by  $E_c = T\xi_c(T)$  and hence we can now plot  $I(E_c)$  versus  $E_c$  near the Fermi level. Finally we can then compare the experimentally derived  $I(E_c)$  with a theoretical expression such as Eq. (15) to obtain the only adjustable parameter, the width  $\Delta$  of the Coulomb gap, as shown in Table II. Note that  $\Delta$  is not used in the analysis to obtain  $I(E_c)$ ; it is a parameter to quantify the width of the Coulomb gap and the density of states. A knowledge of  $\Delta$  also allows one to calculate  $g(E_F)$ . Note that the values of  $g(E_F)$  are fairly similar for the three samples processed from the Ge-2 boule, as might be expected since the carrier concentration varies only slightly between them. Let us estimate  $g(E_F)$  from other considerations. If we assume that all impurities with a concentration  $N$  are distributed randomly and uniformly within an energy interval  $W$ , where  $W$  is the width of the impurity band, then  $g(E_F) = N/W$ . In our case, close to the MIT, the value of  $W$  is comparable with  $\varepsilon_1$ , the energy of ionization of localized electrons to the bottom of the conduction band. Near the MIT in Ge, the value of  $\varepsilon_1$  is  $5 \times 10^{-3}$  eV.<sup>16</sup> Since  $N = 3 \times 10^{17}$  cm<sup>-3</sup>, this gives  $g(E_F) = 6 \times 10^{19}$  cm<sup>3</sup> eV<sup>-1</sup> or  $5 \times 10^{15}$  cm<sup>-3</sup> K<sup>-1</sup> which is close to the values in Table I. The errors in the estimates of  $g(E_F)$  are about 10% and the difference between the three *n*-Ge samples is probably not significant, given that the carrier concentration is similar and close to the metal-insulator transition. For sample H19 (*p*-Ge) the value of  $g(E_F)$  is distinctly higher; for intermediate compensation close to 0.5 the energy distribution of impurities increases outside the Coulomb gap.<sup>1</sup>

The method described above was used also for data in nonzero magnetic field, using  $\xi_c(B, T) = \ln[R(B, T)/R_0]$ . However, we have now to take into account that in strong magnetic fields the electron wave function  $\Psi(r)$  changes its shape from a sphere to a double paraboloid, as studied by Ioselevich.<sup>17</sup> He showed that the critical volume around each site  $V(\xi_c)$ , which in zero field is given by Eq. (10), should be changed in a magnetic field to

$$V(\xi_c) = 8\pi \left[ \frac{2E_0}{m\omega^2} \right]^{3/2} F(\xi_c \hbar \omega / 4E_0), \quad (19)$$

where  $E_0 = \hbar^2 / 2ma^2$  is the binding energy of a localized site,  $\omega = eB/m$  is the cyclotron frequency, and

FIG. 5. The function  $X(s)$ .

$$F(s) = \int_{\tau(s)}^s [\tanh(x/2)(\sinh x + x - 2s) + (s - x)x] \times \frac{(\sinh x + x - 2s)^{1/2} x \sinh x}{(\sinh x - x)^{5/2}} dx, \quad (20)$$

where  $\tau(s)$  is the solution of

$$\sinh x + \tau - 2s = 0.$$

Following Schoepe,<sup>18</sup> Eq. (19) can be rewritten using the reduced variables  $\xi^* = \xi_c(B, T)/\xi_c(0, T)$  and  $B^* = B/B_c$ , where  $B_c = 6\hbar/ea^2\xi_c(0, T)$ . By introducing a new function  $X(s)$ ,

$$X(s) = 6F(s)/s^3, \quad (21)$$

we obtain Eq. (19) in a form which is more convenient to compare with Eq. (10):

$$V(\xi_c) = \frac{4\pi}{3} \left[ \frac{a\xi_c}{2} \right]^3 X(3\xi^*B^*). \quad (22)$$

From a comparison of Eqs. (10) and (22) it follows that the deviation from the spherical shape of the wave function can be taken into account by using the function  $X(s)$ , which is plotted in Fig. 5. According to Eq. (11),  $I(E_c) \sim 1/V(\xi_c)$ , therefore in a magnetic field we obtain  $I(E_c)$  from the experimental data using

$$I(E_c) = \frac{6n_c}{\pi} \frac{1}{a^3} \frac{1}{(\xi_c(B, T))^3} \frac{1}{X(3\xi^*B^*)}, \quad (23)$$

where, as before, the energy scale is given by  $E_c = T\xi_c(B, T)$ . Note that large values of  $E_c$  correspond to high temperatures and magnetic fields and it is this regime, rather than the low-temperature limit, which must be investigated for evidence of crossover phenomena. The results of this procedure are shown in Figs. 6(a)–6(d) where the integrated density of states is normalized as  $I^*(E_c) = I(E_c)/2g_0\Delta^3$  and is plotted against  $E_c/\Delta = x$ . With this normalization procedure the integrated density of states for a pure Coulomb gap is given by  $I^*(E_c) = x^3/3$  while with a finite gap, half-width  $\Delta$ , this becomes  $I^*(E_c) = [x - \arctan(x)]$  from Eq. (15). By plotting the integrated density of states normalized in this

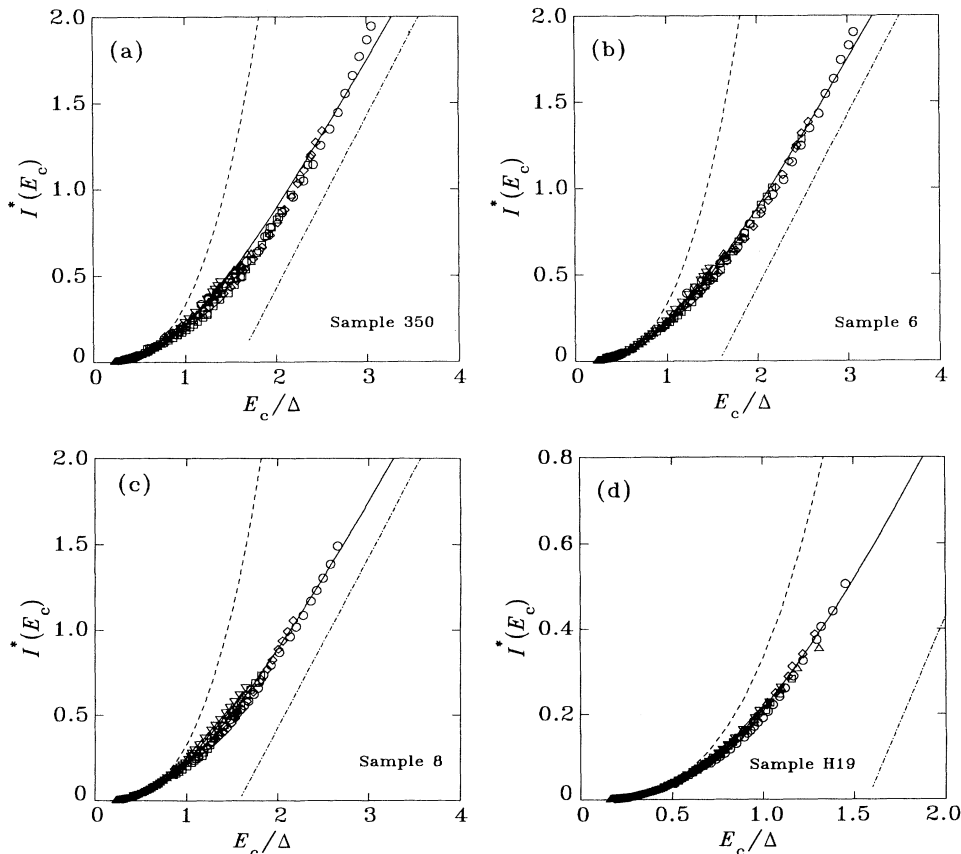


FIG. 6. The normalized integrated density of states  $I^*(E_c)$  for samples 350 (a), 6 (b), 8 (c), and H19 (d), plotted versus  $E_c/\Delta$ . The symbols correspond to zero magnetic field ( $\triangle$ ) and fields of 1 ( $\nabla$ ), 3 ( $\square$ ), 5 ( $\diamond$ ), and 7 ( $\circ$ ) T. The solid line shows Eq. (15), the dashed line Eq. (16), and the dot-dashed line Eq. (17).

TABLE III.  $a(B)/a(0)$  for Ge samples at 5 and 7 T.

Sample	Field	5 T $a(B)/a(0)$	7 T $a(B)/a(0)$
350		0.93	0.88
6		0.95	0.91
8		0.95	0.91
H19		0.96	0.92

way it is possible to describe the VRH conductivity in all magnetic fields and for all samples by a universal curve  $I^*(E_c)$ .

In order to fit the experimental data at the highest magnetic fields (5 and 7 T) we had to slightly reduce the values of  $a(B)$  as shown in Table III, while keeping  $R_0$  and  $\Delta$  constant. This effect could be explained as a result of the shrinkage of the electronic wave function in strong magnetic fields. Decreasing  $a$  means that the magnetic field moves the sample further from the MIT and therefore the values of  $\kappa$  are also changed according to the scaling relation  $\kappa(B)/\kappa(0)=[a(B)/a(0)]^2$ . Hence  $g_0$  is decreased as follows from Eq. (4) and this is allowed for in the normalization. The variation of  $a(B)$  is in good agreement with that proposed by Schoepe.<sup>8</sup> A final point here is that  $\Delta$  may also scale as some power of  $a(B)$  and hence depend on the magnetic field. We have tried using various empirical scaling relations of the form  $\Delta(B)/\Delta(0)=[a(0)/a(B)]^z$  in the data analysis. For  $z > 0$  good fits to the universal function can also be obtained but only by introducing a slightly increasing and field-dependent  $R_0(B)$ .

One can see also from Fig. 6 that the stronger the magnetic field the further from the CG regime are the experimental points. This is in agreement with the conclusion in Ref. 3 that strong magnetic fields reduce the effectiveness of the Coulomb gap. However the deviations from the CG regime depend on the values of  $\Delta$  as can be seen by comparing samples 6 and H19. A knowledge of  $g_0$  and  $\Delta$  allows us to calculate the DOS around the Fermi energy. The DOS for all samples are shown in Fig. 7. One can see that for sample H19 with a large CG and large  $g(E_F)$  the interval of energies where

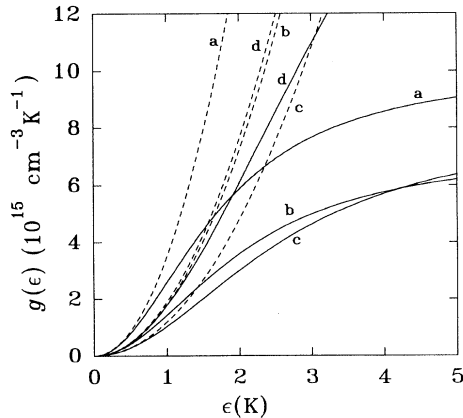


FIG. 7. The DOS  $g(\epsilon)$  near the Fermi level for samples 350 (a), 6 (b), 8 (c), and H19 (d). The dashed lines show the “pure” Coulomb gap  $g(\epsilon)=g_0\epsilon^2$ .

the DOS is close to the parabolic CG is more extended. These ideas can be used to explain why the exponent  $p$  in the resistivity, Eq. (1), remains close to 0.5 at all magnetic fields.

Finally we would like to comment on the field dependence of the magnetoresistance as expressed in the exponent  $q$  in the expression

$$\ln \left[ \frac{R(B)}{R(0)} \right] = \left[ \frac{B}{B_0} \right]^q. \quad (24)$$

At low fields  $q=2$ , as shown in Figs. 2(a) and 2(b). In the high-field limit,  $q$  should ultimately decrease to a value of  $\frac{1}{3}$  for a constant density of states or  $\frac{1}{5}$  for a Coulomb gap.<sup>18</sup> According to the sub-barrier scattering model, proposed by Shklovskii,<sup>19</sup>  $T_{1/2} \approx B^{1/2}$  in strong fields. One can see that all theoretical models predict values of  $q$  less than unity. Nevertheless, experiment shows that  $q \approx 1$  in high fields (Fig. 4). The reason for this is not yet clear but the field dependence of  $a(B)$  gives increased magnetoresistance and hence increases  $q$  as defined in Eq. (24).

In Ref. 20 an interpretation of the nonlinear behavior of  $\ln R$  versus  $T^{-1/2}$  in NTD Ge was suggested in terms of the possible influence of spin-spin interactions which would lead to a  $T^{-1}$  law in the low-temperature limit as observed in irradiated polymer films and amorphous alloys. It is now clear that the low-temperature limit in NTD Ge (at least down to 30 mK) is determined by the Coulomb gap at the Fermi level and deviations from the  $T^{-1/2}$  law with increasing temperature are due to the crossover to a constant DOS. Very similar data to that reported here have recently been published by Dai, Zhang, and Sarachik<sup>21</sup> in Si:B, showing all the features of a crossover from a constant DOS to the CG regime, though in the low-temperature limit they observed an activated conductivity with  $\ln \rho \propto 1/T$ . An alternative analysis following the procedure described here is given in Ref. 22.

In conclusion we wish to discuss the previous observations of the crossover phenomenon in VRH conductivity which were claimed in a number of publications (see Ref. 10 in Ref. 3). In some of these works deviations from a straight line  $\ln R$  vs  $T^{-1/2}$  to lower resistance values (i.e., below the straight line) with increasing temperature have been observed. In our opinion, deviations to higher resistance (i.e., above the straight line) must be observed, because the DOS in the crossover regime is less than for the “pure” parabolic gap (see Fig. 7). Just such deviations were observed and discussed in the present work.

#### ACKNOWLEDGMENTS

We would like to thank Professor E. E. Haller for the H19 sample and details of its preparation. We are grateful to Professor M. Kaveh and Dr. E. Kogan for fruitful discussions.

- <sup>1</sup>For a review, see B. I. Shklovskii and A. L. Efros, *Electronic Properties of Doped Semiconductors* (Springer-Verlag, Berlin, 1984).
- <sup>2</sup>See, for example, *Hopping Transport in Solids*, edited by M. Pollak and B. I. Shklovskii (Elsevier, Amsterdam, 1991).
- <sup>3</sup>I. Shlimak, M. Kaveh, M. Yosefin, M. Lea, and P. Fozooni, *Phys. Rev. Lett.* **68**, 3076 (1992).
- <sup>4</sup>H. Fritzsche and M. Cuevas, *Phys. Rev.* **119**, 1238 (1960); E. E. Haller, N. P. Palaio, and M. Rodder, in *Proceedings of the Fourth International Conference on Neutron Transmutation Doping of Semiconducting Materials*, edited by R. D. Larabee (Plenum, New York, 1984); N. P. Palaio, S. J. Pearton, and E. E. Haller, *J. Appl. Phys.* **55**, 1437 (1984).
- <sup>5</sup>I. S. Shlimak, L. I. Zarubin, A. N. Ionov, F. M. Vorobkalo, A. G. Zabrodskii, and I. Yu. Nemish, *Pis'ma Zh. Tekh. Fiz.* **9**, 877 (1983) [*Sov. Tech. Phys. Lett.* **9**, 377 (1983)].
- <sup>6</sup>C. M. Lederer and V. S. Shirley, *Table of Isotopes*, 7th ed. (Wiley, New York, 1978).
- <sup>7</sup>A. N. Ionov, M. N. Matveev, and D. V. Shmikk, *Zh. Tekh. Fiz.* **59**, 169 (1989) [*Sov. Phys. Tech. Phys.* **34**, 691 (1989)].
- <sup>8</sup>W. Schoepe, *Z. Phys. B* **71**, 455 (1988).
- <sup>9</sup>According to V. L. Nguen, B. Z. Spivak, and B. I. Shklovskii [*Pis'ma Zh. Eksp. Teor. Fiz.* **41**, 35 (1985) [*JETP Lett.* **41**, 42 (1985)] sub-barrier scattering in VRH should lead to negative magnetoresistance (NM) in weak fields. For this NTD Ge no NM was observed down to sufficiently low temperatures. Therefore we have based our analysis on I. S. Shlimak, A. N. Ionov, and B. I. Shklovskii, *Fiz. Tekh. Poluprovodn.* **17**, 503 (1983) [*Sov. Phys. Semicond.* **17**, 314 (1983)] where the sub-barrier scattering was not taken into account.
- <sup>10</sup>A. Ionov, I. Shlimak, and M. Matveev, *Solid State Commun.* **47**, 763 (1983).
- <sup>11</sup>E. Abrahams, P. Anderson, D. C. Licciardello, and T. V. Ramakrishnan, *Phys. Rev. Lett.* **42**, 673 (1979).
- <sup>12</sup>Y. Imry, Y. Gefen, and D. J. Bergman, in *Proceedings of the Taniguchi Symposium*, edited by Y. Nagaoka (Springer-Verlag, Berlin, 1982).
- <sup>13</sup>A. N. Ionov, M. J. Lea, and R. Rentzsch, *Pis'ma Zh. Eksp. Teor. Fiz.* **54**, 470 (1991) [*JETP Lett.* **54**, 473 (1991)].
- <sup>14</sup>B. I. Shklovskii and I. S. Shlimak, *Fiz. Tekh. Poluprovodn.* **6**, 129 (1972) [*Sov. Phys. Semicond.* **6**, 104 (1972)].
- <sup>15</sup>A. Aharony, Y. Zhang, and M. P. Sarachik, *Phys. Rev. Lett.* **68**, 3900 (1992).
- <sup>16</sup>E. A. Davis and W. D. Compton, *Phys. Rev.* **140**, A2183 (1965).
- <sup>17</sup>A. S. Ioselevich, *Fiz. Tekh. Poluprovodn.* **15**, 2373 (1981) [*Sov. Phys. Semicond.* **15**, 1378 (1981)].
- <sup>18</sup>H. Tokumoto, R. Mansfield, and M. J. Lea, *Philos. Mag.* **46**, 93 (1982).
- <sup>19</sup>B. I. Shklovskii, *Fiz. Tekh. Poluprovodn.* **17**, 2055 (1983) [*Sov. Phys. Semicond.* **17**, 1311 (1983)].
- <sup>20</sup>I. S. Shlimak, in *Hopping and Related Phenomena* (World Scientific, Singapore, 1990), pp. 49–59.
- <sup>21</sup>P. Dai, Y. Zhang, and M. P. Sarachik, *Phys. Rev. Lett.* **69**, 1804 (1992).
- <sup>22</sup>I. S. Shlimak and M. J. Lea (unpublished).